V ENCONTRO NACIONAL DE CIÊNCIAS TÉRMICAS - São Paulo,SP - BRASIL (DEZ. 1994)
II SIMPÓSIO DE ENGENHARIA TÉRMICA - SP - BRASIL (DEZ. 1994)

NUMERICAL STUDY OF THE TURBULENT FLOW IN A BIFURCATING CHANNEL USING A MULTIDOMAIN PROCEDURE

J. F. V. Vasconcellos and C. R. Maliska

SINMEC – Laboratory of Computational Fluid Dynamics
Mechanical Engineering Department – UFSC
P. O. Box 476 - 88040-900 - Florianópolis - SC – Brazil

SUMMARY

Bifurcating ducts occurs in a wide range of engineering applications. The motivation for this work is the need of better understanding the turbulent flow in a bifurcating channel encountered in the wire enamelling process. Due to the nature of the channel geometry the use of boundary-fitted coordinates which maps onto a single retangular domain is unfeasible. Therefore, a multidomain technique is developed where velocity and pressure information from one domain to another is transfered through the interface. The k-ε turbulent model for high Reynolds number flows is employed.

INTRODUCTION

Bifurcating ducts occur in a wide range of engineering applications, such as hydraulic and ventilation systems, heat exchangers, chemical processing plants and residential hot water plumbing. Several variations in flow configuration, like a 90° tee, a 45° branch, or a symmetric "Y" branch with combinig or dividing flows, are possible. Although many arrangements are employed in practice, the objective of this work is to present a multidomain method applied to a special type of geometry and flow configuration encountred in the industrial oven where enamelled wire is manufactured.

Numerous representative reports of studies on bifurcation flows have appeared in the literature. Dimitriadis (1986) predicted the three-dimensional turbulent flowfield in junctions consisting of ducts with retangular cross-section using both numerical and experimental methods. Three-dimensional computation of turbulent flow in a tee-junction with wall heat and mass transfer is shown in Pollard (1981) and in Pollard and Spalding (1978) where they performed a numerical study of a splitting flow in a similar geometry. Three-dimensional flows was also computed by Samagaio and Vlachos (1989) which shows the three-dimensional flow produced in the recirculating regions of tee-junctions. Kawaguti and Hamano (1979) studied the two-dimensional low Reynolds flow in a channel with variable angle branch. Bramley and Sloan (1987) performed a numerical study of "Y" branch using boundary-fitted coordinates. Hayes *et alli* (1989) studied the flow characteristics of a Newtonian fluid in a two-dimensional right angled tee-branch by solving the Navier-Stokes equations using the finite element method.

The present work is based on the numerical solution of the two-dimensional form of the time-averaged constant-property Navier-Stokes equations with the goal at developing a multidomain algorithm to deal with a broad class of bifurcating channels. Turbulent viscosity is defined by the high Reynolds number version of the k-ε model of turbulence (Launder and Spalding, 1974).

MATHEMATICAL MODEL

The conservation equations written for general coordinate systems (ξ,η) for a generic scalar ϕ is

$$\frac{\partial(\rho U\phi)}{\partial\xi}+\frac{\partial(\rho V\phi)}{\partial\eta}=\frac{\partial}{\partial\xi}\left(c_1\Gamma\frac{\partial\phi}{\partial\xi}\right)+\frac{\partial}{\partial\eta}\left(c_2\Gamma\frac{\partial\phi}{\partial\xi}\right)+\frac{\partial}{\partial\xi}\left(c_2\Gamma\frac{\partial\phi}{\partial\eta}\right)+\frac{\partial}{\partial\eta}\left(c_4\Gamma\frac{\partial\phi}{\partial\eta}\right)+S^{\phi}-P^{\phi} \tag{1}$$

where

$$U=uy_\eta-vx_\eta \qquad V=vy_\xi-ux_\xi$$
$$J=(x_\xi y_\eta-x_\eta y_\xi)^{-1} \qquad c_1=J(x_\eta x_\eta+y_\eta y_\eta) \tag{2}$$
$$c_2=-J(x_\eta x_\xi+y_\eta y_\xi) \qquad c_4=J(x_\xi x_\xi+y_\xi y_\xi)$$

with P^{ϕ} given by

$$P^{\phi}=y_\eta\frac{\partial P^*}{\partial\xi}-y_\xi\frac{\partial P^*}{\partial\eta} \quad \text{when} \quad \phi=u \tag{3}$$

$$P^{\phi}=x_\xi\frac{\partial P^*}{\partial\eta}-y_\eta\frac{\partial P^*}{\partial\xi} \quad \text{when} \quad \phi=v \tag{4}$$

$$P^{\phi}=0 \quad \text{when} \quad \phi=1,\ \mathrm{k},\ \epsilon \tag{5}$$

ϕ	Γ	S^{ϕ}
1	0	0
u	μ_{ef}	$\frac{\partial}{\partial\xi}[J\mu_{ef}y_\eta(y_\eta\frac{\partial u}{\partial\xi}-x_\eta\frac{\partial v}{\partial\xi})+J\mu_{ef}y_\xi(y_\eta\frac{\partial u}{\partial\eta}-x_\eta\frac{\partial v}{\partial\eta})]+$ $\frac{\partial}{\partial\eta}[J\mu_{ef}y_\eta(x_\xi\frac{\partial v}{\partial\xi}-y_\xi\frac{\partial u}{\partial\xi})+J\mu_{ef}y_\xi(x_\xi\frac{\partial v}{\partial\eta}-y_\xi\frac{\partial u}{\partial\eta})]$
v	μ_{ef}	$\frac{\partial}{\partial\xi}[J\mu_{ef}x_\eta(x_\eta\frac{\partial v}{\partial\xi}-y_\eta\frac{\partial u}{\partial\xi})+J\mu_{ef}x_\xi(x_\eta\frac{\partial v}{\partial\eta}-y_\eta\frac{\partial u}{\partial\eta})]$ $\frac{\partial}{\partial\eta}[J\mu_{ef}x_\eta(y_\xi\frac{\partial u}{\partial\xi}-x_\xi\frac{\partial v}{\partial\xi})+J\mu_{ef}x_\xi(y_\eta\frac{\partial u}{\partial\eta}-y_\xi\frac{\partial v}{\partial\eta})]$
k	$\mu_L+\frac{\mu_T}{\sigma_k}$	$P_k^T-\rho\epsilon$
ϵ	$\mu_L+\frac{\mu_T}{\sigma_\epsilon}$	$\frac{\epsilon}{k}(C_1P_k^T-C_2\rho\epsilon)$

Table 1: Values of Γ and S^{ϕ} Eq. (1)

The ϕ variable represents the mass conservation equation, the two cartesian time mean velocity components in the x and y directions – u and v, respectively –, the turbulent kinetic energy, k, and its dissipation, ϵ. P^* is the local effective pressure in the mean-flow momentum equations. The values of Γ, S^{ϕ} and P^{ϕ} are summarized

in Table 1. The constants in the k-ϵ model are those proposed by Launder and Spalding (1974).

With reference to Table 1, the effective viscosity, μ_{ef}, is calculated from the local values of the turbulence kinetic energy, k, and its dissipation rate, ϵ via

$$\mu_{ef} = \mu_L + \mu_T = \mu_L + \frac{C_\mu \rho \mathrm{k}^2}{\epsilon} \tag{6}$$

where μ_L, μ_T and μ_{ef} are respectively molecular, turbulent and effective viscosities.

The volumetric generation rate of turbulence, P_{k}^T, written in the (ξ,η) coordinate system is :

$$P_{\mathrm{k}}^T = \mu_T J \left[\left[\frac{\partial}{\partial \xi}(v y_\eta - u x_\eta) - \frac{\partial}{\partial \eta}(u x_\xi - v y_\xi) \right]^2 + 2\left[\frac{\partial}{\partial \xi}(u y_\eta) - \frac{\partial}{\partial \eta}(u y_\xi) \right]^2 + 2\left[\frac{\partial}{\partial \eta}(v x_\xi) - \frac{\partial}{\partial \xi}(v x_\eta) \right]^2 \right] \tag{7}$$

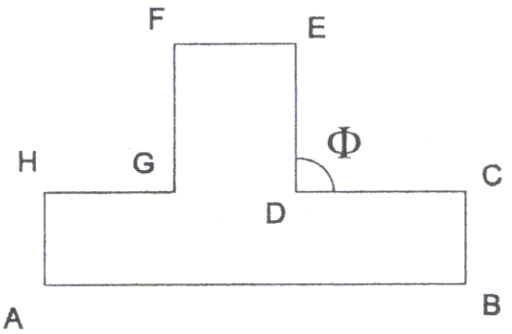

Figure 1: Bifurcation Geometry

BOUNDARY CONDITIONS

Inlet Boundaries

On the inlet planes, $\overline{AH}$ and $\overline{BC}$ section in Fig. 1, all dependent variables – except pressure – are prescribed as

$$u = U_{inlet} \qquad v = 0 \qquad \mathrm{k} = 10^{-3} U_{inlet}^2 \qquad \epsilon = \frac{\mathrm{k}^{1.5}}{H} \tag{8}$$

where H is the length $\overline{AH}$ and U_{inlet} is a function of the Reynolds number. The Reynolds number is defined as $\rho U_{inlet}/H$.

Outlet Boundary

On the outlet plane, $\overline{EF}$ section in Fig. 1, the derivative of all dependent variables – except pressure – are prescribed as

$$\frac{\partial u}{\partial x} = \frac{\partial v}{\partial x} = \frac{\partial \mathrm{k}}{\partial x} = \frac{\partial \epsilon}{\partial x} = 0 \tag{9}$$

where x in Eq. (9) is the direction normal to the $\overline{EF}$ section.

Walls

On the wall planes – $\overline{AB}$, $\overline{CD}$, $\overline{DE}$, $\overline{DE}$, $\overline{FG}$ and $\overline{GH}$ sections in Fig. 1, the artificial boundary condition known as wall function is applied. The wall functions that had been used in this work are the same that can be seen in Hackman's thesis (1982) and are given by

$$v = 0 \tag{10}$$

At the wall, w, the shear stress, τ_w, are given by :

$$\tau_w = (\mu + \mu_T)\frac{du}{dy} = \begin{cases} \dfrac{\rho u \kappa C_\mu^{\frac{1}{4}} \mathrm{k}^{\frac{1}{2}}}{ln(Ey^+)} & \text{se} \quad y^+ > 11.63 \\ \dfrac{\mu_L u}{y} & \text{se} \quad y^+ \leq 11.63 \end{cases} \tag{11}$$

and the dimensionless distance from the wall, y^+, is

$$y^+ = y\frac{C_\mu^{\frac{1}{4}} \mathrm{k}^{\frac{1}{2}}}{\mu_L} \tag{12}$$

where $\kappa = 0.4187$ e $E = 9.793$.

The turbulence energy dissipation rate is :

$$\epsilon = \frac{C_\mu^{\frac{3}{4}} \mathrm{k}^{\frac{3}{2}}}{\kappa y} \tag{13}$$

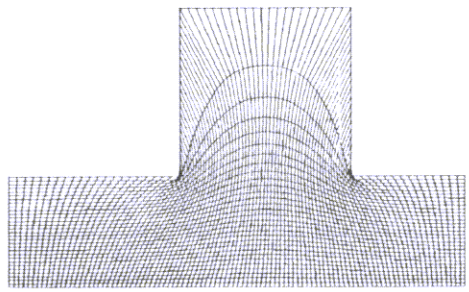

Figure 2: Boundary-fitted coordinates applied in a tee-branch

NUMERICAL PROCEDURE

A finite volume method (Patankar, 1980) using nonorthogonal grids with co-located variables is used to formulate the approximations to the differential equations of this problem. The difficulty associated with the use of co-located variables was removed using the numerical approximation of the pressure gradients proposed by Marchi and Maliska (1994) based on Peric's work (1988).

The SIMPLEC method of Van Doormall and Raithby (1984) is employed for treating the pressure-velocity coupling. The five systems of algebric equations are solved by an ADI procedure as discribed in Silva *et alli* (1993).

Boundary-fitted coordinates were used to discretize all differential equations. This methodology has been used to handle a wide range of geometric configurations. Therefore, for geometries with protuberances, as in Fig. 2, it is not easy to find a coordinate system with maps onto a single rectangle. A much better approach to handle this geometry is to segment into two simple geometries instead of using only a single domain.

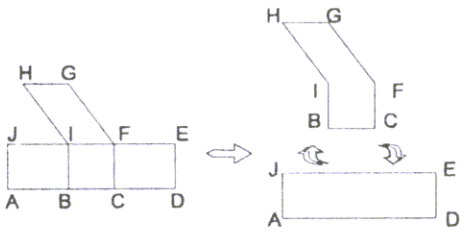

Figure 3: Bifurcation geometry and its two subdomains

Fig. 3 shows how the bifurcation geometry is transformed into two domains which are easier to apply the boundary-fitted methodology. Since the two domains are linked, there must exist a relation between each grid. The grid in the $\overline{IFCB}$ region must be the equal for both domains.

The Eq. (1) is solved for each subdomain. But the actual boundary condition is not available for all subdomain. When the code is solving the horizontal domain, the boundary conditions on $\overline{IF}$ is unknown, and when the code is solving the vertical domain, the boundary conditions on $\overline{IB}$ and $\overline{CF}$ are also unknowns. In the vertical domain, both section $\overline{IB}$ and $\overline{CF}$ are available because they are interior section in the horizontal domain. This situation is equivalent for the $\overline{IF}$ boundary, which is a boundary in the vertical domain, but is an interior section in the vertical domain.

The multidomain procedure algorithm is therefore :

1. ϕ is estimated for each variable and each subdomain;
2. Horizontal subdomain – Eq. (1) is solved for each ϕ. The value of ϕ on the $\overline{IF}$ boundary should be get from the ϕ on the vertical subdomain;
3. Vertical subdomain – Eq (1) is solved for each ϕ. The value of ϕ on the $\overline{IB}$ and $\overline{CF}$ boundaries should be get from the ϕ on the horizontal subdomain;
4. The step 2 and 3 must be repeated until the convergence of both subdomains is reached.

Changing a boundary-fitted single domain code into a boundary-fitted multidomain is not too difficult. The single domain code must be a subroutine of a multidomain algorithm shown before.

One of the convergence criteria adopted is related with mass residuals. First the absolute mass residual for each finite volume is calculated and this value is divided by the mass-flow of the section. This value should be smaller than 0.01% for all cells. Second, none of the ϕ variables on the unknown boundaries must change by more than 1% between two sucessive cicles.

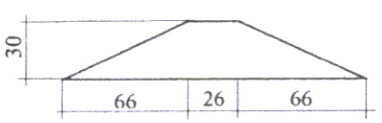

Figure 4: Bump dimensions [mm]

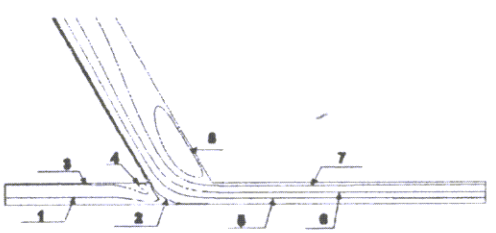

Figure 5: Streamlines for the first geometry

The turbulence model was compared with the Stephenson (1975) work, where two-dimensional turbulent flow in parallel plates is predict by the use of a finite-difference solution procedure. The Reynolds number, definid on bulk velocity ($2\rho u_b L/\mu$) is 140,000. The spacing between the parallel plates, L, is 0.051 [m]. These plates are 3.66 long and the grid used to solve this problem is 60×48. The result is shown in Fig. 6 where the dots are Stephenson's results and y is the distance from the plates centreline. The results agree well except along the centreline.

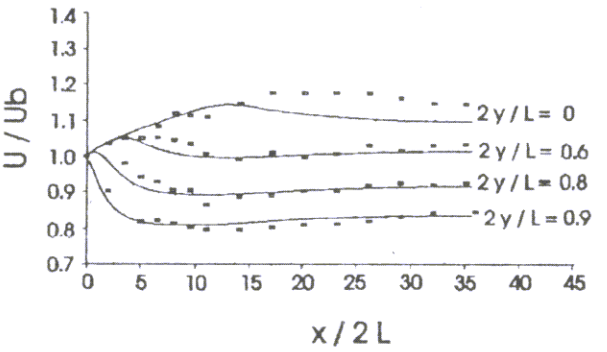

Figure 6: Two-dimensioanl turbulent flow beteween parallel plates

The multidomain procedure was compared with the results of Kawaguti and Hamano (1979). Fig. 7 shows the grid used to compute laminar flow in a 30° bifurcation. Fig. 8 shows the streamlines of the Kawaguti and Hamano results (upper) and the streamlines obtained in this work. Further details about the multidomain procedure can be find in Vasconcellos (1993).

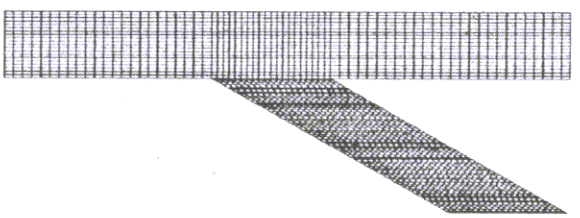

Figure 7: Bifurcation grid 82×22 (horizontal) and 22×82 (vertical)

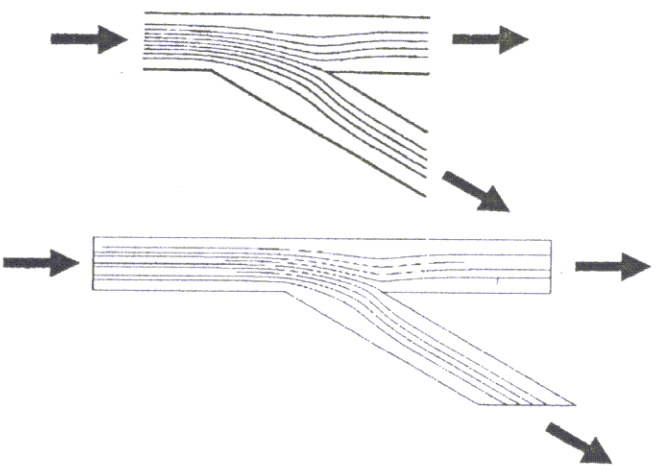

Figure 8: Streamlines in a 30° bifurcation

RESULTS AND CONCLUSIONS

The computations presented herein comprise two geometries of combining-flow mode. The first geometry reproduces the situation where the bifurcation angle, Φ, is 60^o and without bumps in the horizontal domain. The second reproduces the situation where $\Phi = 90^o$ and with four bumps in the horizontal domain. The bumps helps to create a flow where heat and mass trasfer is enhanced. For the enameling process this is of almost importance Both calculations were performed for Reynolds number equal 63,781 - $\mu = 1.846 \times 10^{-5}$ [kg /ms] and $\rho = 1.1774$ [kg /m^3] - and were carried out with 120×16 (horizontal domain) and 32×62 (vertical domain) meshes. This grid was chosen after a grid dependence study. The bifurcation dimensions are : $\overline{AH} = 70$ [mm], $\overline{FE} = 200$ [mm], $\overline{AB} = 1500$ [mm], $\overline{HG} = 450$ [mm] and $\overline{DE} = 450$ [mm]. Fig. 4 shows the bump dimensions. The first upper bump is located at 689 [mm] from the left side of the bifurcation while the second at 1,061 [mm]. The first lower bump is located at 862 [mm] from the left side of the bifurcation while the second at 1,260 [mm]. The left inlet mass flow is $v_w = 0,05\ [\frac{m^3}{s}]/m$ and the right inlet mass flow is $v_e = 0,95\ [\frac{m^3}{s}]/m$.

Fig. 5 and Fig. 9 show the streamlines for the first and second case, respectively. For these problems no experimental data could be found in the open literature.

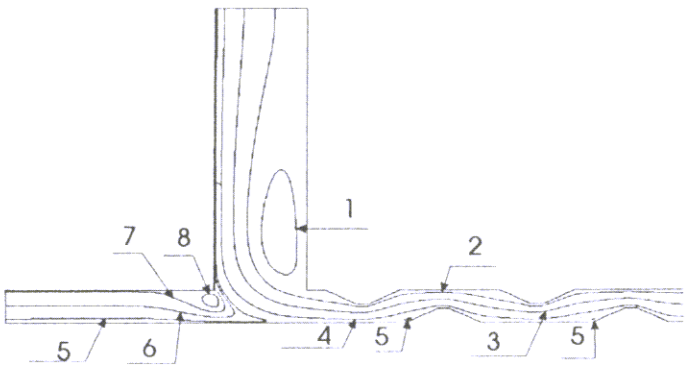

Figure 9: Streamlines for the second geometry

Number	Streamlines 1st case	Streamlines 2nd case
1	$1.743\ 10^{-2}$	$-1.079\ 10^{0}$
2	$-7.276\ 10^{-3}$	$-8.797\ 10^{-1}$
4	$4.864\ 10^{-2}$	$-1.487\ 10^{-1}$
3	$5.920\ 10^{-2}$	$-5.310\ 10^{-1}$
5	$-2.502\ 10^{-1}$	$6.527\ 10^{-3}$
6	$-5.451\ 10^{-1}$	$2.814\ 10^{-2}$
7	$-8.607\ 10^{-1}$	$5.092\ 10^{-2}$
8	$-1.035\ 10^{0}$	$6.675\ 10^{-2}$

Table 2: Streamlines - Fig. 5 and Fig. 9

It was demonstrated with tge tests presented in this paper that the use of boundary-fitted grids with a multidomain technique is an attractive alternative for solving fluid flow problems in complex geometries.

REFERENCES

- Bramley, J. S. e Sloan, D. M., *"Numerical Solution for Two-Dimensional Flow in a Branching Channel Using Boundary-Fitted Coordinates"*, **Computers & Fluids**, Vol. 15, pp. 297–311, 1987.
- Dimitriadis, K. P., *"Computation of Three-Dimensional Turbulent Flow in Nonorthogonal Junctions"*, **Ph.D. Thesis**, Manchester Universitv. Manchester. England. 1986.
- Hackman, L. P., *"Numerical Study of the Turbulent Recirculating Flow over a Backward-Facing Step Using a Two Equation Turbulence Model"*, **Ph.D. Thesis**, University of Waterloo, Waterloo, Canada, 1982.
- Hayes, R. E. *et al.*, *"Steady Laminar Flow in a 90 Degree Planar Branch"*, **Computers & Fluids**, Vol. 17, pp. 537–553, 1989.
- Kawaguti, M. e Hamano, A., *"Numerical Study on Bifurcating Flow of a Viscous Fluid"*, **Journal of the Physical Society of Japan**, Vol. 46, pp. 1360–1365, 1979.
- Launder, B. E. e Spalding, D. B., *"The Numerical Computation of Turbulent Flows"*, **Computer Methods in Applied Mechanics and Engineering**, Vol. 3, pp. 269–289, 1974.
- Marchi, C. H. and Maliska, C. R, *"A Nonorthogonal Finite Volume Method for Solution of All Speed Flows Using Co-Located Variables"*, **Numerical Heat Transfer**, Accepted for publication, 1994.
- Patankar, S. V., *"Numerical Heat Transfer and Fluid Flow"*, **Hemisphere Publishing**, 1980.
- Peric, M., Kessler, R. e Scheuerer, G., *"Comparison of Finite Volume Numerical Methods with Staggered and Colocated Grids"*, **Computers & Fluids** , Vol. 16, pp. 389–403, 1988.
- Pollard, A., *"Computer Modelling of Flow in Tee-Junctions"*, **Physic Chemical Hydrodynamics**, Vol. 2, pp. 203–227, 1981.
- Pollard, A. e Spalding, D. B., *"The Prediction of the Three-Dimensional Turbulent Flow Field in a Flow-Splitting Tee-Junction"*, **Computer Methods in Applied Mechanics and Engineering**, Vol. 13, pp. 293–306, 1978.
- Samagaio, A. e Vlachos, N. S. *"Calculation of Three-Dimensional Laminar Flows in T-Shaped Junctions"*, **Computer Methods in Applied Mechanics and Engineering**, Vol. 75, pp. 393–407, 1989.
- Silva, A. F. C., Marchi, C. H., Livramento, M. A. and Azevedo, J. L.F., *"On the Effects of Vectorization for Efficient Computation of Three-Dimensional Segregated Finite Volume Solutions"*, **XI Proceedings of the XI ABCM Mechanical Engineering Conference**, pag. 109-112, São Paulo, S ao Paulo, Brasil, 1991.
- Stephenson, P. L., *"A Theoretical Study of Heat Transfer in Two-Dimensional Turbulent Flow in a Circular Pipe and Between Parallel and Diverging Plates"*, **Internatioanl Journal of Heat and Mass Transfer**, Vol. 19, pp. 413–423, 1989.
- Van Doormaal, J. P. e Raithby, G. D., *"Enhancements of the SIMPLE Method for Predicting Incompressible Fluid Flow"*, **Numerical Heat Transfer**, Vol. 7, pp. 147–163, 1984.
- Vasconcellos, J. F. V., *"Simulação Numérica de Escoamento Turbulento em Bifurcação usando Multidomínios"*, **Dissertação de Mestrado**, Universidade Federal de Santa Catarina, Florianópolis, Brazil, 1993.

ACNOWLEDGMENTS

The partial financial support to J. F. V. de Vasconcellos by Conselho Nacional de Desenvolvimento Científico e Tecnológico (CNPq) and Pirelli Industrial Brasileira S/A is gratefully acknonowledged.